Engineering Innovations
ISSN: 2813-1002, Vol. 11, pp 1-8
doi:10.4028/p-qvAF50

Submitted: 2023-12-10
Revised: 2024-01-02
Accepted: 2024-01-03
Online: 2024-06-26

Simulation of Stress Intensity Factor and J-Integral on UIC 54 Railway Failure Using A Fracture Mechanics Approach

Pradhana Kurniawan[1,a*], Darto Darto[1,b], Agus Iswantoko[1,c], Feliks Sutrisno[2,d]

[1]Mechanical Engineering Department, Faculty of Engineering, University of Merdeka Malang, Terusan Dieng Street No. 62-64 Klojen, Pisang Candi, Malang, East Java 65146, Indonesia

[2]Department of Mechanical and Industrial Engineering, Faculty of Engineering, State Universty of Malang, Semarang Street 5, Lowokwaru, Malang, Eas Java, Indonesia

[a]pradhana.kurniawan@unmer.ac.id, [b]darto@unmer.ac.id, [c]agus.iswantoko@unmer.ac.id, [d]mazmur118@gmail.com

Keywords: Stress Intensity Factor, J-Integral, Crack Defects, Railroads, Fracture Mechanics.

Abstract. Repeated loading on the railroad tracks will result in fatigue failure. Fatigue failure combined with a defect in the form of a crack in the railroad track will result in a decrease in strength. Defects in the form of cracks are formed due to improper manufacturing and treatment processes. One treatment that can cause the formation of defects in the form of cracks is thermite welding. Improper and non-standard thermite welding techniques can trigger the formation of defects in the form of cracks in the railroad joints. Based on these problems, this simulation aims to obtain information about the value of maximum stress, SIF, J-Intergal, number of cycles, and crack extension from variations in crack size to repeated loading. The method consists of preprocessing, processing and postprocessing. Preprocessing begins with the design of the UIC 54 railroad crack which consists of 3 variations of crack length, namely 10 mm, 15 mm, and 20 mm. The design was tested through static structural simulation using the ANSYS 2021 R2 application. Meshing is configured using an element size of 5 mm and uses curvature capture. The results of the simulation obtained maximum stress values, SIF, J-Integral, number of cycles, and crack extension. Based on the simulation of SIF 1 and J-Integral values on the specimen design with a crack length of 10 mm it shows 362.03 Mpa.mm$^{1/2}$ of 0.5708 mJ/mm^2, for an initial crack length of 15 mm that is equal to 482.81 Mpa.mm$^{1/2}$ and 0.91738 mJ/mm^2, and for an initial crack length of 20 mm, it is 600.54 Mpa.mm$^{1/2}$ and 1.4465 mJ/mm^2. The results show that the increase in SIF 1 and J-Integral will be proportional to the increase in the initial crack length value.

Introduction

Rails serve as a path of rail transportation. Railroad rails have various types that are adjusted based on the type of train [1]. Coal transport type trains pass through the UIC 54 type railroad [2]. UIC 54 rail is the type of rail used for coal transport trains in the South Sumatra area of Indonesia.

Repetitive loading of the rail combined with the presence of defects will result in fatigue failure. Based on the classification, the railway (UIC 54) is included in class I where the rail transport capacity is 2 x 10^6 tons/year. Each train car carries coal with a coal load capacity of around 50 tons and the carriages have a separate load of 22 tons. The transport train passes through a railroad connection, where the technique used to connect the railroad tracks is using thermite welding. Thermite welding has a weakness that can be a factor in the occurrence of railroad faults [3], [4]. These weaknesses include low ductility and toughness, rough surface grains, dendritic structure, inclusions, and the formation of porosity. Porosity or the presence of holes in the connecting parts between the rails is the cause of cracks and fractures on railway tracks [2]. Thermite welding, which is a heat treatment technique, can cause changes in mechanical properties including strength, hardness, ductility and toughness [5]–[7].

Research on failure due to fatigue where the high speed of the train affects the condition of the railway track UIC 54. The high speed of the train moving over the track can trigger unsafe conditions for the railroad track. Failure due to fatigue can occur without a sign so that cracks that eventually

result in fractures can occur. The loading occurs in the direction perpendicular to the crack surface, where the stages begin with initiation, propagation and finally cracking [8], [9]. A similar study is concerned with the fracture toughness of high-speed rail in Malaysia. The Tanah Melayu Berhad (KTMB) train runs on UIC 54 railroad tracks with 900A class steel used on Electrical System Train (ETS) train tracks. Loading on train tracks will produce bending stress, axial stress, and Hertzian pressure during contact with the train track. These stresses can trigger failure when there are defects in the railroad tracks [10].

Based on several previous studies which discussed the toughness of railway tracks against repeated loading which produces fatigue. This research aims to simulate variations in crack length with respect to SIF 1 and J-Integral values due to loading from coal trains. The simulation was carried out using ANSYS 2021 R1 software with the fatigue method to obtain information regarding the maximum stress, SIF, J-Integral, number of cycles, and crack extension that occurred on the UIC 54 railway track. The simulation was carried out on the design of the UIC 54 railway track. with a length of 100mm. Variations in crack length are given in the design, namely 10 mm, 15 mm, and 20 mm, with the same crack height, namely 1 mm.

Methods

Pre-processing. The research began with design modeling in the form of the UIC 54 railroad track. The design modeling of the UIC 54 railroad track was carried out using the Inventor application. There are 3 types of designs that will be used in testing through simulation. Information regarding the design used in the simulation based on the size of the crack is shown in Table 1 and Figure 1.

Table 1. Specimen Crack Design and Size

Specimen	Crack Type	Crack Length (mm)	Crack Height (mm)
1	*Single edge crack*	10	1
2	*Single edge crack*	15	1
3	*Single edge crack*	20	1

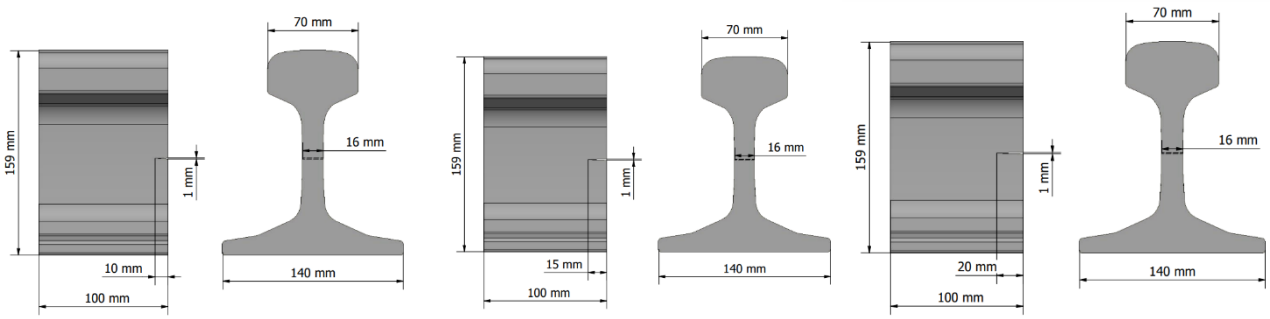

Fig. 1. Geometry of the UIC 54 Railway Tracks with Crack Lengths (a) 10 mm (b) 15 mm and (c) 20 mm

After the UIC 54 railroad track design process is determining the properties of the materials used by the UIC 54 railroad track. Configuration of the properties of the UIC 54 railroad track is done via ANSYS 2021 R2 software. The mechanical properties of the UIC 54 railroad are shown in Table 2.

Table 2. UIC 54 Railway Specifications [2], [8], [10]

Characteristics	Value
Young Modulus	210 GPa
Poisson's Ratio	0,29
Bulk Modulus	166,67 GPa
Shear Modulus	81,395GPa
Tensile Yield Strength	879 Mpa
Tensile Ultimate Strength	948 MPa
Coefficient of Thermal Expansion	$2{,}3 \times 10^{-5}\ C^{-1}$
Material Constant C (Paris Law)	$1{,}31935 \times 10^{-12}$ (mm, tonne mm s^{-2})
Material Constant m (Paris Law)	3,2825 (mm, tonne mm s^{-2})

After inputting the UIC 54 rail material into the engineering data, the next process is meshing. Crack coordinate configuration needs to be done to set the direction in which the crack occurs. The Y-axis configuration has a direction perpendicular to the surface of the UIC 54 train track that will contact the train wheels. The X axis has a direction parallel to the movement of the train wheels. The crack coordinate configuration is shown in Figure 2. The meshing stages were carried out with the configuration shown in Table 3 and the results are in Figure 3.

Table 3. Meshing Configuration

Parameter	Configuration
Element size	5 mm
Capture Curvature	*Yes*
Method	*Tetrahedrons*
Edge Sizing	*Sphere radius* 9 mm, *Element size* 1 mm, *Sphere Center* (*crack coordinate system*)

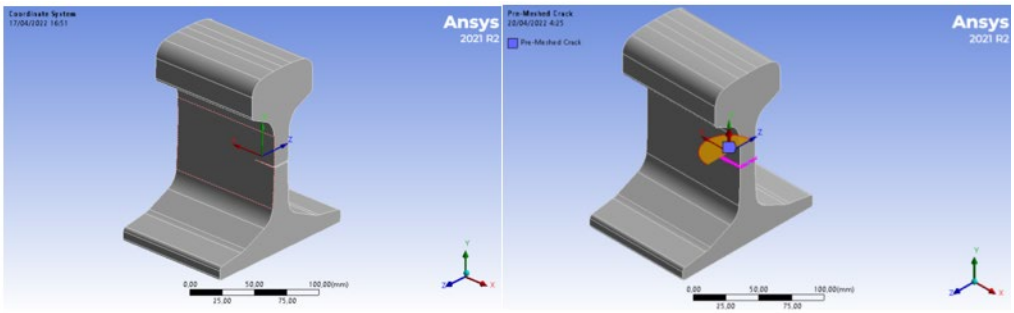

Fig. 2. (a) Coordinate System Configuration for Crack Propagation and Crack Direction Configuration

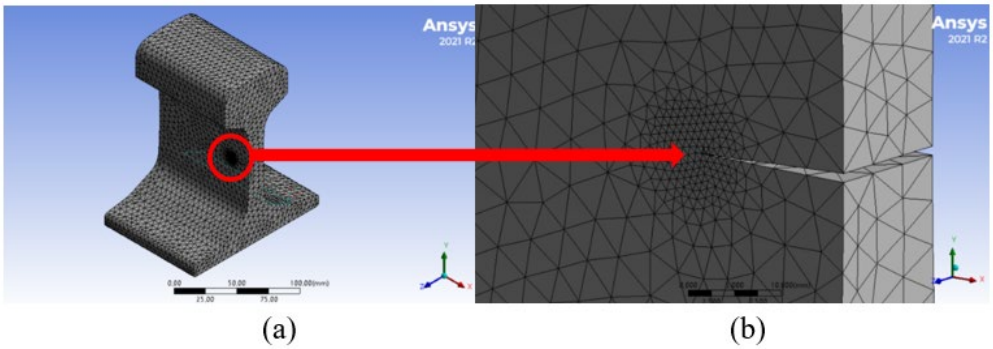

Fig. 3. (a) Meshing configuration and (b) Meshing configuration on the crack section

After meshing, the next process is adding fracture features and configuring cracks using pre-meshed cracks accompanied by smart crack growth. Previously, named selection was performed to create a nodal named selection, which is required as one of the parameters in the pre-meshed crack configuration. There are 3 named selections, namely at the ends of the 2 cracked surfaces, the upper cracked surface area, and the lower cracked surface area. The next step is to select a nodal named selection at the ends of the 2 cracked surfaces as crack fronts. Activate the crack faces nodes and select the top face nodes and bottom face nodes as the top face nodes and bottom face nodes. The coordinate system is set based on the configuration that has been previously set from Figure 3. Next, do the configuration for smart crack growth where the configuration uses fatigue settings. Crack initiation is selected based on the previous configuration of the pre-meshed crack. The material used is a material whose properties have been configured as shown in Table 2.

The analysis configuration stage begins by determining the number of steps that are configured in 1 stage with a time of 1 second. The crack control configuration is set alternately, you can do an analysis based on SIF first then J-Integral or vice versa. Next, set the part that becomes the fixed support and the location where the contact occurs for the force from the railroad wheels to the UIC 54 railroad as shown in Figure 5. The loading on the UIC 54 railroad 100 mm long is regulated by a train that has a load consisting of a body trains, boogies, and transported products. Based on research regarding failure in the form of fractures on the UIC 54 train tracks due to loading from coal trains [1]. The largest load is on the part of the carriage that transports coal products, namely 77 tons. The load is the load from one coal train car carrying coal. The direction of the load is perpendicular to the surface of the UIC 54 railway track which is the route of the coal carrying train. There are 2 UIC 54 railroad tracks that support the load of one coal carriage and there are 2 boogies in one carriage. Each boogie consists of 4 train wheels, so that each side of the train track has 4 train wheels. The loading of the train is explicitly explained in Table 4 and Figure 5. Based on Table 4, the load of one wheel on one side of the rail is 94421.25 N.

Table 4. Distribution of the Train Load on the UIC 54 Railroad

Railway Section	Value	Load
Coal wagons and their transport	1	77000 kg (77 ton)
Boogie	2	38500 kg by one boogie
Wheels on Every Boogie	4	9625 by one wheel

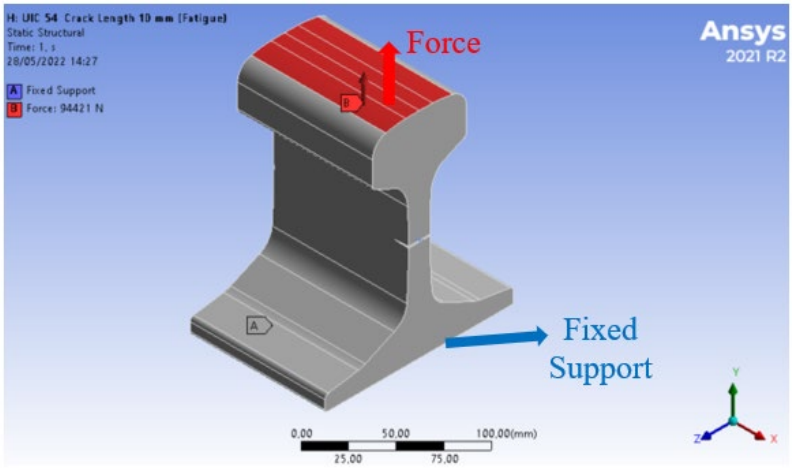

Fig. 4. Boundary Conditions

Processing. Processing is a computational process that works to solve predetermined and configured problems. The computing system will solve problems based on the problems and the required results.

Post-processing. Post-processing is the result of a simulation in solving predetermined and configured problems. Simulation results include equivalent von misses, Stress Intensity Factor, J-Integral, number of cycles and crack extension.

Results and Discussion

Based on the SIF and J-Integral simulation results for cracks of length 10 mm, 15 mm, and 20 can be seen in Figure 5-7.

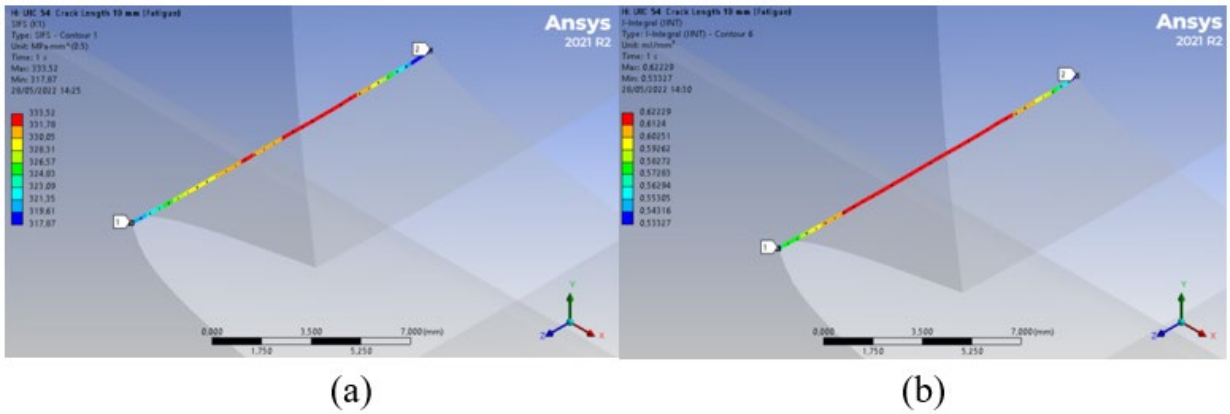

Fig. 5. (a) SIF Mode 1 and (b) J-Integral for Crack Length 10 mm

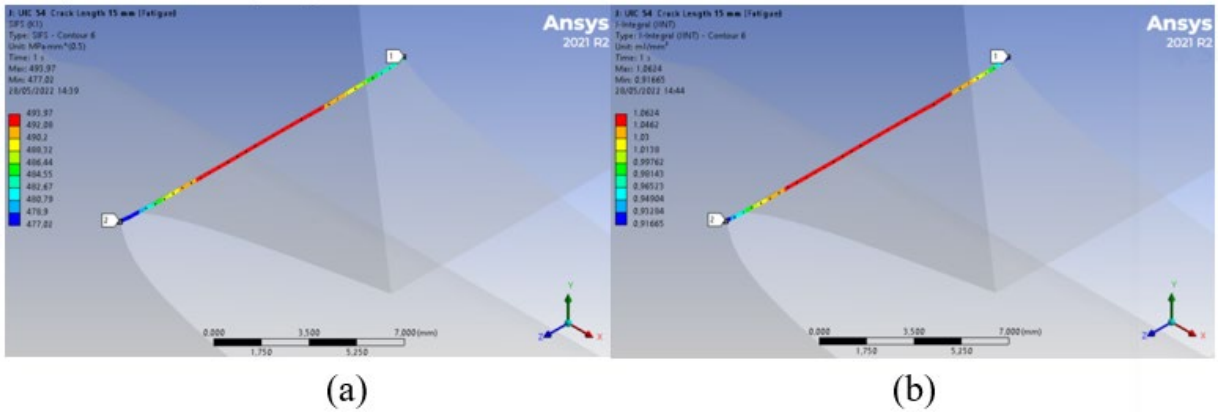

Fig. 6. (a) SIF Mode 1 and (b) J-Integral for Crack Length 15 mm

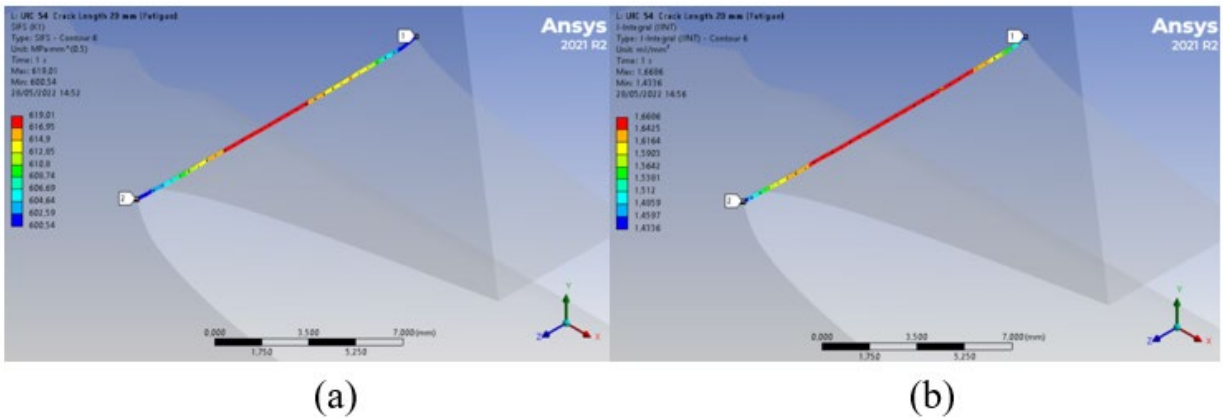

Fig. 7. (a) SIF Mode 1 and (b) J-Integral for Crack Length 20 mm

Table 5. Simulation Data Results

Crack Length	Equivalent Von Misses (MPa)	*Mode* I *of Stress Intesity Factor* (Mpa.mm$^{1/2}$)	J-Integral (mJ/mm^2)	*Number of Cycles*	*Crack Extension* (mm)
10 mm	239,81	362,03	0,5708	3109	0,98492
15 mm	297,96	482,81	0,91738	1431	1,1405
20 mm	382,39	600,54	1,4465	691	1,1568

Based on the results of the simulation in Table 5 and the graphical comparison of crack lengths of 10 mm, 15 mm and 20 mm, namely for maximum stress, SIF mode 1, J-Integral, crack extension, and number cycles. Information can be obtained regarding the effect of crack length on UIC 54 railroad specimens. Figure 8 shows a comparison of the maximum stress values for 3 different specimens. The highest maximum stress is found in a crack with a length of 20 mm which is 382.39 Mpa, followed by a crack with a length of 15 mm and finally a crack with a length of 10 mm which is respectively 297.96 Mpa and 239.81Mpa. The stress value increases with the increase in the initial value of the crack is directly proportional to the value [11]. As the SIF value increases as the initial length of the crack increases, the stress value will also increase. This is in accordance with the equation for determining the SIF value [12].

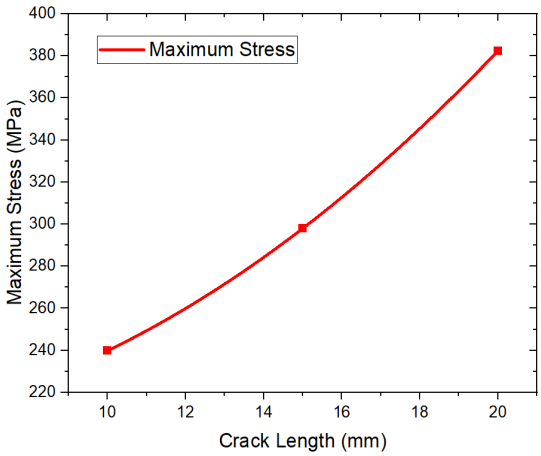

Fig. 8. Equivalent Von Misses Comparison of Crack Lengths 10 mm, 15 mm, and 20 mm

Figure 9 shows a comparison of SIF mode 1 and J-Integral values on 3 different specimens. Specimens with a crack length of 20 mm had the highest SIF 1 and J-Integral values, namely 600.54 Mpa.mm$^{1/2}$ and 10.225 mJ/mm^2 respectively. SIF 1 and J-Integral values were followed by specimens with a crack length of 15 mm and the lowest was for specimens with a crack length of 10 mm. SIF 1 and J-Integral values for 15 mm crack length respectively are 482.81 Mpa.mm$^{1/2}$ and 0.91738 mJ/mm^2. The SIF 1 and J-Integral values for a crack length of 10 mm respectively are 362.03Mpa.mm$^{1/2}$ and 0.5708mJ/mm^2. The value of the specimen with a crack length of 20 mm is the highest compared to the specimen with a crack length lower than 20 mm indicating that the greater the crack length with the same crack height, the value of SIF mode 1 and J-Integral will increase [11]. The value of SIF mode 1 and J-Integral which increases with the value of the length of the crack with the same height is also related to the maximum stress value, where the equation for determining the value of SIF 1 and J-Integral is directly proportional to the stress [13]. Increased SIF 1 and J-Integral values also affect the condition of the number of cycles [14].

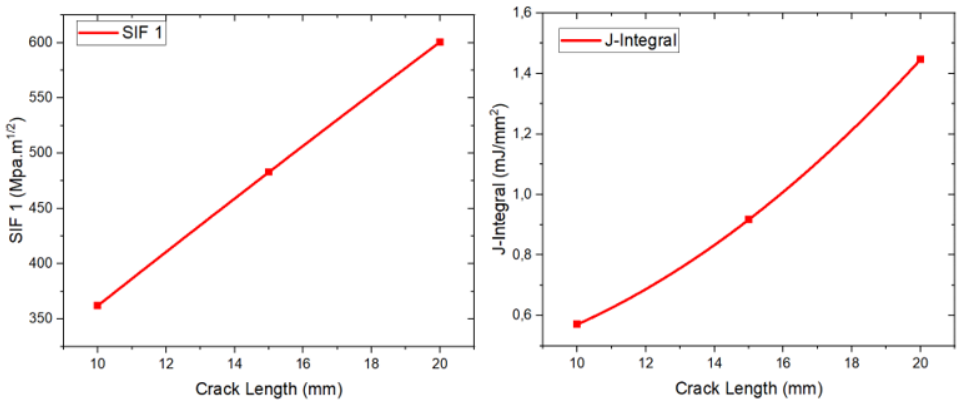

(a) (b)

Fig. 9. Comparison of Crack Lengths 10 mm, 15 mm, and 20 mm for Values of (a) SIF Mode I and (b) J-Integral

Figure 10 is a comparison of the number of cycles of 3 different specimens. Specimens with a crack length of 10 mm have a higher number of cycles than specimens with a crack length of 15 mm and 20 mm. Specimens with a crack length of 10 mm have a number of cycles value of 3109, followed by specimens with a crack length of 15 mm and 20 mm respectively, namely 1431 and 691. Based on the value of the number of cycles at the same time it shows that the longer the cracks on the specimen the UIC 54 railroad, the age of the railroad will decrease [14]. The decreasing number of cycles value indicates that the size of the defect in the specimen has a greater length and/or width, thus affecting the age of the specimen. The decreased number of cycles value indicates that the voltage value increases [11].

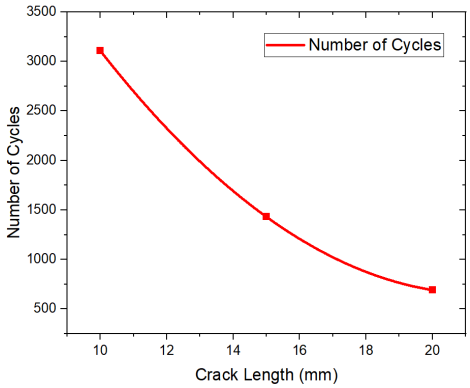

Fig. 10. Comparison of Number of Cycles for Crack Lengths of 10 mm, 15 mm, and 20 mm

Figure 11 is a comparison of the crack ekstension from 3 different specimens. Based on Table 5, the value of the increase in crack length in the specimen with a crack length of 20 mm experienced an increase in crack length of 1.1568 mm. Specimens with a crack length of 15 mm experienced an increase in crack length of 1.1405 mm, and for specimens with a crack length of 20 mm experienced an increase in crack length of 0.98492 mm. The increase in crack length is influenced by the value of the initial crack length and SIF [15]. The greater the value of the initial length of the crack, the more the SIF value increases, the value of the increase in crack length will increase. Based on Figure 9, the value of the increase in crack length increases when the initial length of the crack is 10 mm to 15 mm, and begins to decrease when the initial length of the crack is more than 15 mm. This shows that the speed of crack propagation has a maximum speed when the initial length of the crack is more than 15 mm to 20 mm.

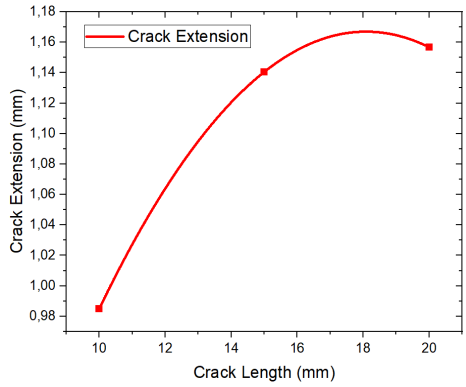

Fig. 11. Comparison of Crack Ekstension for Crack Lengths of 10 mm, 15 mm, and 20 mm

Summary

The aim of this simulation is to analyze the SIF, J-integral, equivalent von misses, number of cycles and crack extension in the failure of the UIC 54 railway track. The highest stress result is 382.39 MPa at a crack length of 20 mm. The increase in stress value is directly proportional to SIF (600.54 MPa.mm$^{1/2}$), J-Integral (1.4465 mJ/mm^2), Number of Cycles (691 cycles) and Crack Extensions (1.1568 mm). This condition can be concluded that the greater the value of the initial crack length with the same crack height, the greater the value of SIF mode 1 and J-Integral. A large

initial crack length value will also have a lower lifespan compared to specimens that have a shorter crack length. The increase in crack length will increase along with the increase in the initial length of the crack until at a certain size it will reach the condition of maximum propagation speed.

References

[1] T. A. Zucarelli, M. A. Vieira, L. A. Moreira Filho, D. A. P. Reis, and L. Reis, "Failure analysis in railway wheels," *Procedia Structural Integrity*, vol. 1, pp. 212–217, 2016, doi: 10.1016/j.prostr.2016.02.029.

[2] A. Ihlas, "Analysis of Damage to Coal Transport Rail Rails," *Journal of Materials and Engineering Goods Technology*, vol. 7, p. 7, Jun. 2017, doi: 10.37209/jtbbt.v7i1.89.

[3] S. Kwon, D.-H. Lee, S. Kwon, and B. Goo, "Failure Analysis of Railway Wheel Tread," *Key Engineering Materials - KEY ENG MAT*, vol. 321–323, pp. 649–653, Oct. 2006, doi: 10.4028/www.scientific.net/KEM.321-323.649.

[4] G. Fedorko, V. Molnár, P. Blaho, J. Gašparík, and V. Zitrický, "Failure analysis of cyclic damage to a railway rail – A case study," *Engineering Failure Analysis*, vol. 116, p. 104732, Oct. 2020, doi: 10.1016/j.engfailanal.2020.104732.

[5] A. Andoko and P. Puspitasari, "The Fatigue Crack Growth Rate Due to Single-Step Austempered Heat Treatment in Nodular Cast Iron," *MATEC Web Conf.*, vol. 97, p. 01028, 2017, doi: 10.1051/matecconf/20179701028.

[6] Pradhana, A. Andoko, and P. W. Sunu, "Leaf spring type simulation with finite element method approach," *IOP Conf. Ser.: Mater. Sci. Eng.*, vol. 1034, no. 1, p. 012015, Feb. 2021, doi: 10.1088/1757-899X/1034/1/012015.

[7] D. Darto, "Structural and Thermal Comparative Analysis of Ventilated Disc Brake Discs," in *National Seminar on Technology Faculty of Engineering 2021*, Jan. 2021. [Online]. Available: https://seminar.unmer.ac.id/index.php/sistek/SISTEK/paper/view/637

[8] P. Gurubaran, M. Afendi, M.A.N. Fareisha, M. S. A. Majid, I. Haftirman, and M.T.A. Rahman, "Fatigue life investigation of UIC 54 rail profile for high speed rail," *J. Phys.: Conf. Ser.*, vol. 908, no. 1, p. 012026, Oct. 2017, doi: 10.1088/1742-6596/908/1/012026.

[9] P. Kurniawan and Y. Gemilang, "Crack Simulation on Diesel Engine Crankshaft using Finite Element Method," *TRANSMISI*, vol. 19, pp. 37–40, Mar. 2023, doi: 10.26905/jtmt.v19i1.9800.

[10] M. A. Rojan, M. S. M. Azmi, M. S. A. Majid, R. Daud, and K. S. Basaruddin, "Fracture toughness of railway for higher speed rail corridors in Malaysia," *IOP Conf. Ser.: Mater. Sci. Eng.*, vol. 670, no. 1, p. 012065, Nov. 2019, doi: 10.1088/1757-899X/670/1/012065.

[11] A. Lal, B. M. Sutaria, and K. Mishra, "Fracture analysis of single edge cracked functionally graded material plate under various loading conditions by extended finite element method," *IOP Conf. Ser.: Mater. Sci. Eng.*, vol. 814, no. 1, p. 012014, Mar. 2020, doi: 10.1088/1757-899X/814/1/012014.

[12] T. L. Anderson, *Fracture Mechanics: Fundamentals and Applications, Fourth Edition*, 4 edition. CRC Press, 2017.

[13] M. Aursand and B. H. Skallerud, "Mode I stress intensity factors for semi-elliptical fatigue cracks in curved round bars," *Theoretical and Applied Fracture Mechanics*, vol. 112, p. 102904, Apr. 2021, doi: 10.1016/j.tafmec.2021.102904.

[14] M. Torabizadeh, Z. A. Putnam, M. Sankarasubramanian, J. C. Moosbrugger, and S. Krishnan, "The effects of initial crack length on fracture characterization of rubbers using the J-Integral approach," *Polymer Testing*, vol. 73, pp. 327–337, Feb. 2019, doi: 10.1016/j.polymertesting.2018.11.026.

[15] W. Li, X. Long, S. Huang, Q. Fang, and C. Jiang, "Elevated fatigue crack growth resistance of Mo alloyed CoCrFeNi high entropy alloys," *Engineering Fracture Mechanics*, vol. 218, p. 106579, Sep. 2019, doi: 10.1016/j.engfracmech.2019.106579.